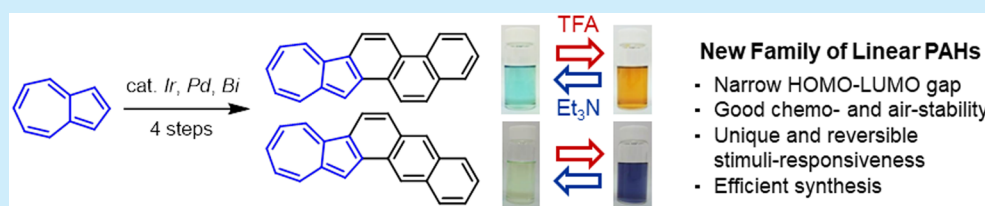


Azulene-Fused Linear Polycyclic Aromatic Hydrocarbons with Small Bandgap, High Stability, and Reversible Stimuli Responsiveness

Masahito Murai,^{*,†} Shinji Iba,[†] Hiromi Ota,[‡] and Kazuhiko Takai^{*,†}

[†]Division of Applied Chemistry, Graduate School of Natural Science and Technology, and [‡]Division of Instrumental Analysis, Department of Instrumental Analysis and Cryogenics, Advanced Science Research Center, Okayama University, 3-1-1 Tsuchimanaka, Kita-ku, Okayama 700-8530, Japan

S Supporting Information



ABSTRACT: Azulene-fused polycyclic aromatic hydrocarbons (PAHs) were synthesized from commercially available azulene in four steps. The resulting azulene conjugates exhibited significantly narrow HOMO–LUMO bandgaps with high air stability, confirmed by photophysical study. Introduction of azulene also enabled the unique reversible stimuli-responsiveness even with the weak acid and base, which can potentially control the degree of conjugation and optoelectronic properties by simple acid–base and redox processes.

The synthesis of functionalized polyaromatic hydrocarbons with extended polycyclic frameworks is of interest because it can produce organic photoelectronic materials for various applications such as field-effect transistors (OFETs), photovoltaics, and light-emitting diodes.¹ For example, linearly fused PAHs, such as pentacene, rubrene, picene, and indeno[1,2-*b*]fluorenes are key components for high-performance OFETs (Figure 1).² These organic semiconducting materials are flexible,

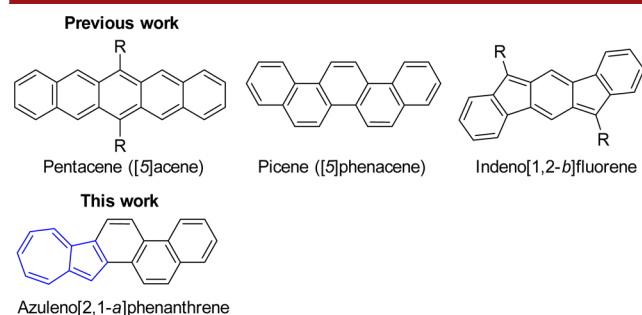


Figure 1. Representative examples of linear PAHs.

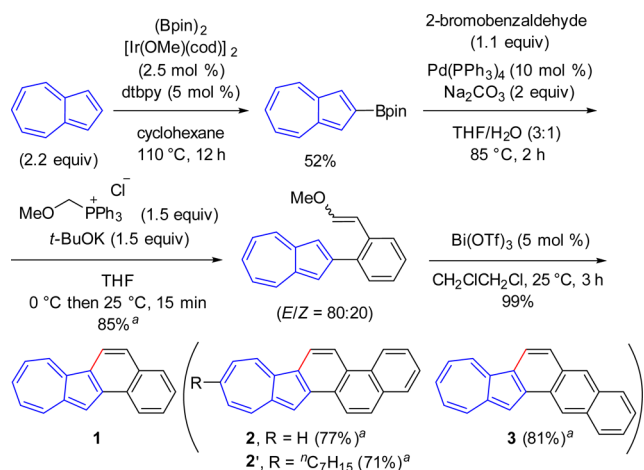
light, and easily shaped compared to transistors based on silicon or other inorganic materials. The properties of these PAHs have been adjusted by taking advantage of the versatility of the chemical synthesis.³ The major strategies can be classified into three categories: (1) introduction of functional groups on the aromatic backbone, (2) incorporation of main group heteroatoms, such as B, N, and P, into the π -conjugated system, and (3) extension of π -systems by annulation with aromatic rings.⁴ These can decrease optical bandgaps, increase electronic

coupling, and control molecular packing to reduce reorganization energies in the solid state. However, PAHs with greater conjugation suffer from intrinsic chemical instability upon exposure to air and light,⁵ and heteroatom-containing substituents sometimes disrupt π -stacking, which inhibits charge carrier transport.⁶ Furthermore, poor solubility derived from intense π – π interactions between the expanded and nonpolar planar π -conjugation systems often limit further applications. To compensate for these drawbacks, there are opportunities for investigations into the design and characterization of unconventional *all carbon* polycyclic aromatic frameworks.⁷ The present study describes the incorporation of an azulene ring⁸ into linearly fused [*n*]acene and [*n*]phenacene structures, i.e., the replacement of two six-membered rings with five- and seven-membered rings, which significantly decrease the bandgaps with retention of stability and solubility. Unique reversible stimuli-responsiveness even with the weak acid and base, which cannot be achieved by incorporation of a naphthalene ring, is also described.

Azulene ring-fused polyaromatic hydrocarbons 1–3 were successfully synthesized in four steps from commercially available azulene (Scheme 1). Iridium-catalyzed C–H bond direct borylation of azulene, conducted using a modification of a procedure by Murafuji et al., afforded a mixture of 2- and 1-borylazulenes in 52% and 23% yield, respectively.⁹ The 2-formylphenyl group was then introduced into the 2-position of azulene via Suzuki–Miyaura cross-coupling reaction of 2-borylazulene. Optimization of the reaction conditions revealed that Pd(PPh₃)₄ and Na₂CO₃ in a mixture of THF and H₂O gave

Received: September 1, 2017

Scheme 1. Synthesis of Azulene-Fused PAHs



^aYields are based on 2-borylazulenes. See the SI for the yield of each step.

the best result for this step. The resulting aldehyde was next converted into the methyl vinyl ether by Wittig reaction. Subsequent bismuth-catalyzed cyclization and aromatization, which was developed by us,¹⁰ proceeded at 25 °C to afford the corresponding naphth[2,1-*a*]azulene (hereafter denoted “NaphAz”) 1 in 99% yield.¹¹ The structure of 1 was unambiguously determined by single-crystal X-ray structure analysis (Figure S9). The stereoisomer ratio of the starting methyl vinyl ether did not affect the efficiency of this cyclization. Azulene derivatives are generally sensitive to acid and oxidant,⁸ and the choice of a mild Lewis acid, Bi(OTf)₃, as a catalyst was key to promoting efficient reaction. Following the same reaction, azuleno[2,1-*a*]phenanthrene (hereafter “PhenAz”) 2 possessing a zigzag structure as well as linear azuleno[2,1-*a*]anthracene (hereafter “AnthAz”) 3 were obtained in 96% and 97% yield, respectively (yield is based on vinyl ethers employed; see the SI for the details). Azuleno[2,1-*a*]phenanthrene 2' with a substituent at the axis position was also obtained in 98% yield. Although pentacenes without any substituents are prone to oxidation and dimerization,⁵ their constitutional isomers, PhenAz 2 and AnthAz 3, were very stable under ambient conditions. The fused azulenes 1–3 were soluble in common organic solvents, such as CH₂Cl₂ and THF, in contrast to the poor solubility of pentacene and picene derivatives.²

To evaluate these azulene-conjugated π -systems as new molecular material candidates, their photophysical properties were determined. The optical data are summarized in Table S1 in SI. The UV–vis absorption spectra of NaphAz 1 was compared with those of chrysene ([4]phenacene) and tetracene ([4]acene) having the same 18 π conjugated system (Figure 2). Three main absorption maxima at 326, 375, and 396 nm and a small shoulder peak near 345 nm were observed for NaphAz 1. These absorptions are similar to those from the parent azulene at 269, 321, and 343 nm, but are red-shifted by more than 50 nm. Additionally, a weak absorption centered at 627 nm, which derived from S₀ \rightarrow S₁ transition and caused the unique blue color of NaphAz 1, was observed. Although the molar absorption coefficient ϵ was low ($\epsilon = 360 \text{ M}^{-1}\text{cm}^{-1}$), blue color derived from the absorption over 600 nm is rare for pure hydrocarbons without any heteroatoms in the neutral state. In contrast, the constitutional isomers chrysene and tetracene produced quite different absorption spectra. The absorption maxima, appearing at 269

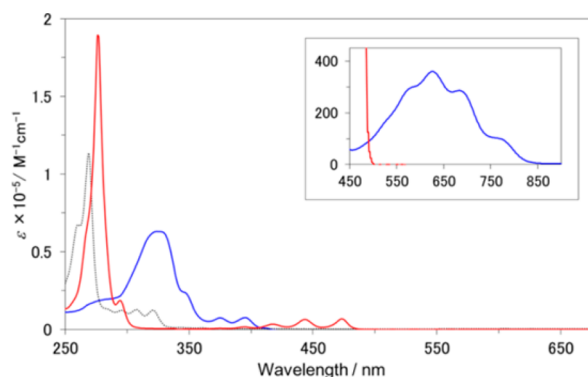


Figure 2. UV–vis spectra of chrysene (black), NaphAz 1 (blue), and tetracene (red) in CH₂Cl₂ at 25 °C. Inset: Enlargement of the absorption in 450–900 nm.

nm for chrysene and 276 nm for tetracene, both were shifted to shorter wavelengths compared with that for NaphAz 1. The optical bandgap of NaphAz 1 obtained from the onset of absorption was estimated to be 1.49 eV. This narrow bandgap of NaphAz 1 is consistent with nonbenzenoid aromatic hydrocarbon systems, such as azulene, which generally have smaller bandgaps than do aromatic systems with the same number of π -electrons.¹²

To gain insight into the structural and electronic properties, density functional theory (DFT) calculations with NaphAz 1, chrysene, and tetracene are conducted using the B3LYP/6-311G(d) level of theory. The entire backbone of NaphAz 1 possesses a highly planar geometry, which correlates well with the structure confirmed by X-ray crystallographic analysis. The electron density distribution of the HOMO orbital of NaphAz 1 is effectively delocalized over the entire backbone, whereas its LUMO orbital is relatively localized on the azulene ring (Figure 3). The HOMO level of NaphAz 1 is higher than chrysene, and

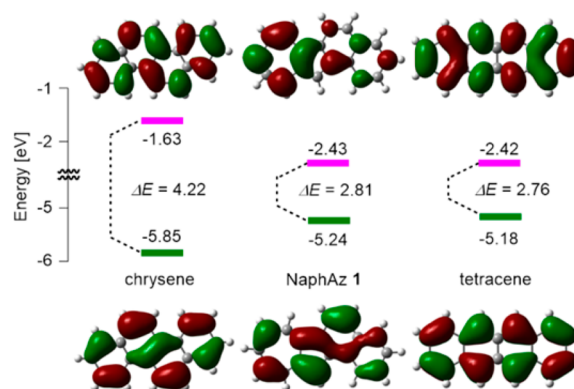


Figure 3. Molecular orbital plots and energy diagrams for chrysene, NaphAz 1, and tetracene calculated using the DFT method at the B3LYP/6-311G(d) level of theory. The values between each level are the energy gaps of the frontier orbital.

nearly identical with tetracene, although the molecular shape is similar to that of chrysene. The HOMO–LUMO energy bandgap of NaphAz 1 estimated from the UV–vis study was smaller than that obtained from DFT calculation (see Figure 2). The parent azulene shows a similar phenomenon (optical bandgap is ca. 1.7 eV, while that estimated from DFT is 3.3 eV). This difference can be rationalized by considering the non-alternant nature of azulene, which generally possess smaller

bandgap than estimated from DFT calculation due to the small repulsive energy between the electrons occupying HOMO and LUMO orbital in the excited state.¹²

It is well-known that exposure of [*n*]acene derivatives in solution to ambient air and sunlight causes oxidative and photolytic degradation.⁵ For example, the half-life of the photooxidation rate for tetracene ([4]acene) was less than 24 h. In sharp contrast, NaphAz 1 was very stable in air and light despite its higher HOMO level and smaller energy bandgap compared with that of [*n*]acene. A decrease in UV absorption intensity was not observed, even when the NaphAz 1 solution was exposed to air and ambient light for 1 day (Figure S2). Furthermore, the NMR spectrum did not indicate any noticeable decomposition, even upon prolonged heating at 150 °C for 1 h. A sample kept in CDCl₃ open to the atmosphere and exposed to ambient light also exhibited no decomposition even after 1 week (see Figure S3 for a similar study for PhenAz 2 and AnthAz 3). In general, stability of PAHs strongly depends on the mode of ring annulation and the topology of their π -electron systems.¹³ The enhanced stability of NaphAz 1 can be rationalized by considering its aromaticity (benzenoid character), i.e. in contrast to NaphAz 1, tetracene is unstable because three double bonds can be drawn in only one ring of its π -system without duplication.

Similar to NaphAz 1, both PhenAz 2 and AnthAz 3 exhibited good stability in air. In addition, the CH₂Cl₂ solution of PhenAz 2 was green and that of AnthAz 3 was yellowish green. The absorption spectrum of AnthAz 3 was similar to that of its isomer PhenAz 2 (Figure 4, solid line), with a strong absorption at 335

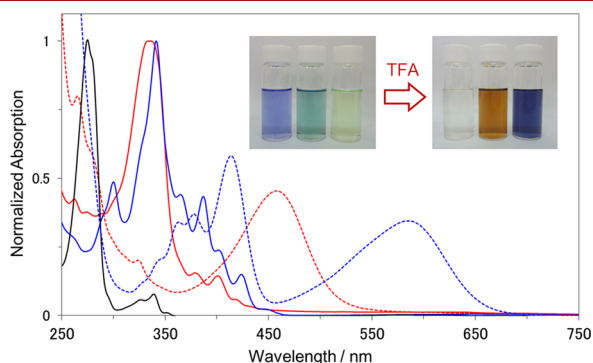


Figure 4. UV-vis spectra of azulene (black), PhenAz 2 (red), and AnthAz 3 (blue) in CH₂Cl₂ in the neutral state (solid line) and after protonation by TFA (dotted line) using TFA/CH₂Cl₂ (v/v = 1/6). Inset: photographs in the neutral state (left) and upon addition of TFA (right).

nm for PhenAz 2 and at 341 nm for AnthAz 3. These absorptions were red-shifted by approximately 10–20 nm compared with NaphAz 1, reflecting extension of π -conjugation. DFT calculations suggested that PhenAz 2 and AnthAz 3 possessed very similar HOMO and LUMO energy levels (Figure S8). Despite similar electronic structures, however, these compounds exhibited completely different stimuli-responsiveness against the acid–base reaction.^{14,15} AnthAz 3 produced a new absorption in the visible region centered at 414 nm with the longest wavelength absorption at 587 nm, while that for PhenAz 2 was only 458 nm upon addition of TFA (Figure 4, dotted line). These absorption changes were accompanied by an instant color change from green to orange (for PhenAz 2) and from yellowish green to dark blue (for AnthAz 3) (see inset in Figure 4). To illustrate the origin of this unusual phenomenon, theoretical calculations of

the excited state for these compounds were conducted using the TD-DFT method at the B3LYP/6-311G(d) level. The calculated absorption spectra agreed well with the experimental spectra (Tables S3–S6). The new absorptions centered at 458 nm for PhenAz 2 and 414 nm for AnthAz 3 are attributed to HOMO–1 \rightarrow LUMO transitions, while that at 587 nm for AnthAz 3 is assigned mainly to the HOMO \rightarrow LUMO transition (oscillator strength $f = 0.1364$) (see Tables S5 and S6). The longest wavelength absorption for PhenAz 2 is attributed to a symmetry–forbidden HOMO \rightarrow LUMO transition with an oscillator strength of 0.0059. HOMO contours existed along the entire annulated π -framework in PhenAz 2 and AnthAz 3 in the neutral state (Figure S8). After protonation, however, HOMO orbitals of PhenAz 2 completely localize on the phenanthrene units, while that of AnthAz 3 delocalize to azulene as well as anthracene moieties (Figure 5). Thus, the distinct differences in

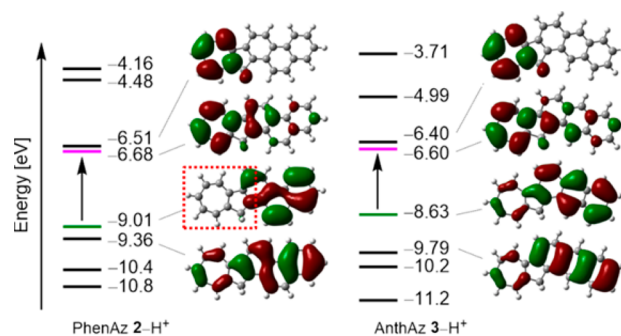


Figure 5. DFT-calculated molecular orbitals and energy diagram of protonated PhenAz 2–H⁺ and AnthAz 3–H⁺.

stimuli-responsiveness observed can be rationalized in terms of the degree of orbital overlap, i.e. HOMO orbital of PhenAz 2 does not overlap effectively with its LUMO, and the absorption derived from this transition has an intramolecular charge-transfer character, which generally has low oscillator strength.

Importantly, neutralization of acidic solutions of PhenAz 2 and AnthAz 3 with triethylamine (Et₃N) regenerated the absorption spectra of their neutral states (Figure 6).¹⁶ The spectral response to these acid–base reactions was very fast, occurring on mixing, and could be repeated for many cycles with no significant variation from cycle to cycle. Reversible change for these compounds could also be monitored by ¹H NMR spectroscopy. Treatment of TFA resulted in the downfield shifts of the

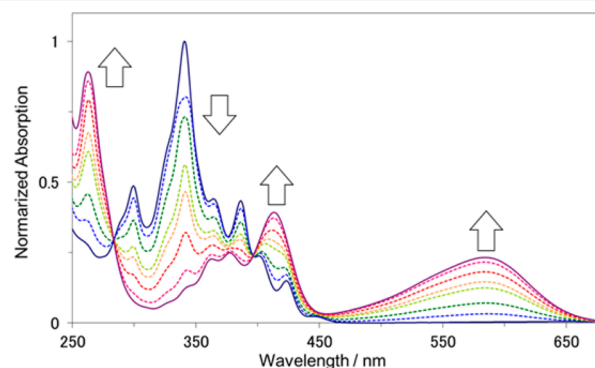


Figure 6. Variation of UV-vis absorption spectra of AnthAz 3 upon the protonation by TFA in CH₂Cl₂ at 25 °C (from neutral state (dark blue line) and after protonation with ca. 15% of TFA (purple line)).

aromatic protons, which were recovered to the initial ^1H NMR spectra in the neutral state by the neutralization with Et_3N (see Figures S6 and S7). In contrast, the original UV-vis spectra of nonsubstituted parent azulene could not be recovered, presumably due to competitive oxidation or decomposition of the protonated azulene species that lack stabilization. The color change shown in Figure 4 also indicated that increase of the number of fused-benzene rings significantly changed the absorption spectra, and makes PhenAz 2 and AnthAz 3 suitable for novel molecular probes for the detection of even weak acid and base by the naked eye.

In conclusion, this study describes facile protocols for the incorporation of azulene rings into PAHs, which affected their photophysical properties. These novel azulene conjugates possessed narrow bandgaps, excellent photooxidative resistance, and good solubility. Blue and green colors in the neutral state derived from absorption in the visible region, as well as unique reversible stimuli-responsiveness, even with a weak acid and base, are rare for pure hydrocarbons without any heteroatoms. These results suggest that azulene-embedded PAHs are promising candidates for novel organic electronic materials. The application of resulting azulene conjugates to OFETs, etc., is ongoing in our laboratory.

■ ASSOCIATED CONTENT

Supporting Information

The Supporting Information is available free of charge on the ACS Publications website at DOI: 10.1021/acs.orglett.7b02729.

Experimental procedures, spectroscopic data for all new compounds, ^1H and ^{13}C NMR spectra, and DFT calculation details (PDF)

X-ray data of compound 1 (CIF)

■ AUTHOR INFORMATION

Corresponding Authors

*E-mail: masahito.murai@okayama-u.ac.jp.

*E-mail: ktakai@cc.okayama-u.ac.jp.

ORCID

Masahito Murai: 0000-0002-9694-123X

Notes

The authors declare no competing financial interest.

■ ACKNOWLEDGMENTS

This work was financially supported by a Grant-in-Aid for Scientific Research (C) (No. 16K05778) from MEXT, Japan, and the Advanced Catalytic Transformation program for Carbon utilization (ACT-C) project of the Japan Science and Technology Agency. M.M. thanks ADEKA Award in Synthetic Organic Chemistry, Japan, and Sumitomo Foundation. We gratefully thank Dr. Sobi Asako, Dr. Hiroki Mori, and Dr. Kazuto Takaishi (Okayama University) for the valuable discussions.

■ REFERENCES

- (1) (a) Anthony, J. E. *Chem. Rev.* **2006**, *106*, 5028. (b) Pron, A.; Gawrys, P.; Zagorska, M.; Djurado, D.; Demadrille, R. *Chem. Soc. Rev.* **2010**, *39*, 2577. (c) Takimiya, K.; Shinamura, S.; Osaka, I.; Miyazaki, E. *Adv. Mater.* **2011**, *23*, 4347.
- (2) For reviews, see: (a) Anthony, J. E. *Angew. Chem., Int. Ed.* **2008**, *47*, 452. (b) Mei, J.; Diao, Y.; Appleton, A. L.; Fang, L.; Bao, Z. *J. Am. Chem. Soc.* **2013**, *135*, 6724. For representative studies on the OFETs application of picones, see: (c) Okamoto, H.; Kawasaki, N.; Kaji, Y.;

Kubozono, Y.; Fujiwara, A.; Yamaji, M. *J. Am. Chem. Soc.* **2008**, *130*, 10470. For indeno[1,2-*b*]fluorenes, see: (d) Chase, D. T.; Fix, A. G.; Kang, S. J.; Rose, B. D.; Weber, C. D.; Zhong, Y.; Zakharov, L. N.; Lonergan, M. C.; Nuckolls, C.; Haley, M. M. *J. Am. Chem. Soc.* **2012**, *134*, 10349.

(3) (a) Alberico, D.; Scott, M. E.; Lautens, M. *Chem. Rev.* **2007**, *107*, 174. (b) Jin, T.; Zhao, J.; Asao, N.; Yamamoto, Y. *Chem. - Eur. J.* **2014**, *20*, 3554.

(4) (a) Qian, G.; Wang, Z. Y. *Chem. - Asian J.* **2010**, *5*, 1006. (b) Weil, T.; Vosch, T.; Hofkens, J.; Peneva, K.; Müllen, K. *Angew. Chem., Int. Ed.* **2010**, *49*, 9068.

(5) (a) Maliakal, A.; Raghavachari, K.; Katz, H.; Chandross, E.; Siegrist, T. *Chem. Mater.* **2004**, *16*, 4980. (b) Kaur, I.; Jia, W.; Kopreski, R. P.; Selvarasah, S.; Dokmeci, M. R.; Pramanik, C.; McGruer, N. E.; Miller, G. P. *J. Am. Chem. Soc.* **2008**, *130*, 16274.

(6) Liu, J.; Walker, B.; Tamayo, A.; Zhang, Y.; Nguyen, T.-Q. *Adv. Funct. Mater.* **2013**, *23*, 47.

(7) (a) Zhu, X.; Tsuji, H.; Navarrete, J. T. L.; Casado, J.; Nakamura, E. *J. Am. Chem. Soc.* **2012**, *134*, 19254. (b) Murai, M.; Maekawa, H.; Hamao, S.; Kubozono, Y.; Roy, D.; Takai, K. *Org. Lett.* **2015**, *17*, 708.

(8) (a) Gordon, M. *Chem. Rev.* **1952**, *50*, 127. (b) Hafner, K. *Angew. Chem.* **1958**, *70*, 419. (c) Nozoe, T. *Pure Appl. Chem.* **1971**, *28*, 239. (d) Xin, H.; Gao, X. *ChemPlusChem* **2017**, *82*, 945. For recent works, see: (e) Murai, M.; Iba, S.; Takai, K. Jpn. Kokai Tokkyo Koho, JP 2015172009 A 20151001, 2015. (f) Yang, X.; Shi, X.; Aratani, N.; Gonçalves, T. P.; Huang, K.-W.; Yamada, H.; Chi, C.; Miao, Q. *Chem. Sci.* **2016**, *7*, 6176.

(9) (a) Kurotobi, K.; Miyauchi, M.; Takakura, K.; Murafuji, T.; Sugihara, Y. *Eur. J. Org. Chem.* **2003**, *2003*, 3663. For iridium-catalyzed silylation of azulene, see: (b) Murai, M.; Takami, K.; Takai, K. *Org. Lett.* **2015**, *17*, 1798. For palladium-catalyzed arylation, see: (c) Murai, M.; Yanagawa, M.; Nakamura, M.; Takai, K. *Asian J. Org. Chem.* **2016**, *5*, 629.

(10) Murai, M.; Hosokawa, N.; Roy, D.; Takai, K. *Org. Lett.* **2014**, *16*, 4134.

(11) Although the synthesis of naphth[2,1-*a*]azulenes having substituents have been reported, there is no study on the relationship between the chemical structures and physical properties. See: Yasunami, M.; Yang, P. W.; Kondo, Y.; Noro, Y.; Takase, K. *Chem. Lett.* **1980**, *9*, 167.

(12) (a) Plattner, P. A.; St. Pfau, A. *Helv. Chim. Acta* **1937**, *20*, 224. (b) Michl, J.; Thulstrup, E. W. *Tetrahedron* **1976**, *32*, 205. (c) Fabian, J.; Zahradnik, R. *Angew. Chem., Int. Ed. Engl.* **1989**, *28*, 677.

(13) Clar, E. *The Aromatic Sextet*; Wiley: London, 1972.

(14) Because UV-vis absorption change occurred in a single step even with excess TFA, monocation might be the plausible species rather than dication, which was generated in the reaction with TFA. Since ESR spectrum of the powder and solution sample showed no signal, generation of azulenumium cation species, which is proposed in the following previous reports, can be ruled out. (a) Wang, F.; Lai, Y.-H.; Kocherginsky, N. M.; Kostecki, Y. Y. *Org. Lett.* **2003**, *5*, 995. (b) Wang, X.; Ng, J.-K.; Jia, P.; Lin, T.; Cho, C. M.; Xu, J.; Lu, X.; He, C. *Macromolecules* **2009**, *42*, 5534.

(15) Azulenes are known to have photophysical properties that are significantly sensitive to pH change. Protonation is reported to occur at the 1- and 3-positions of azulene ring, which resulted in the appearance of the new absorption in the visible and NIR regions derived from its azulenumium cation. For recent examples, see: (a) Murai, M.; Amir, E.; Amir, R. J.; Hawker, C. J. *Chem. Sci.* **2012**, *3*, 2721. (b) Murai, M.; Ku, S.-Y.; Treat, N. D.; Robb, M. J.; Chabiny, M. L.; Hawker, C. J. *Chem. Sci.* **2014**, *5*, 3753. (c) Amir, E.; Murai, M.; Amir, R. J.; Cowart, J. S., Jr; Chabiny, M. L.; Hawker, C. J. *Chem. Sci.* **2014**, *5*, 4483. (d) Tang, T.; Lin, T.; Wang, F.; He, C. *J. Phys. Chem. B* **2015**, *119*, 8176.

(16) See Figures S4 and S5 for variations of the UV-vis absorption spectra of NaphAz 1 and PhenAz 2 upon the protonation by TFA.